Title
A 1-AMPERE, 80 keV LONG PULSE H SOURCE AND ACCELERATOR

Author
Kwan, J.W.

Publication Date
1985-10-01

LBL-20297
Preprint

Lawrence Berkeley Laboratory
UNIVERSITY OF CALIFORNIA

Accelerator & Fusion Research Division

Submitted to Review of Scientific Instruments

A 1-AMPERE, 80 keV LONG PULSE H^- SOURCE AND ACCELERATOR

J.W. Kwan, G.D. Ackerman, O.A. Anderson,
C.F. Chan, W.S. Cooper, G.J. deVries,
A.F. Lietzke, L. Soroka, and W.F. Steele

October 1985

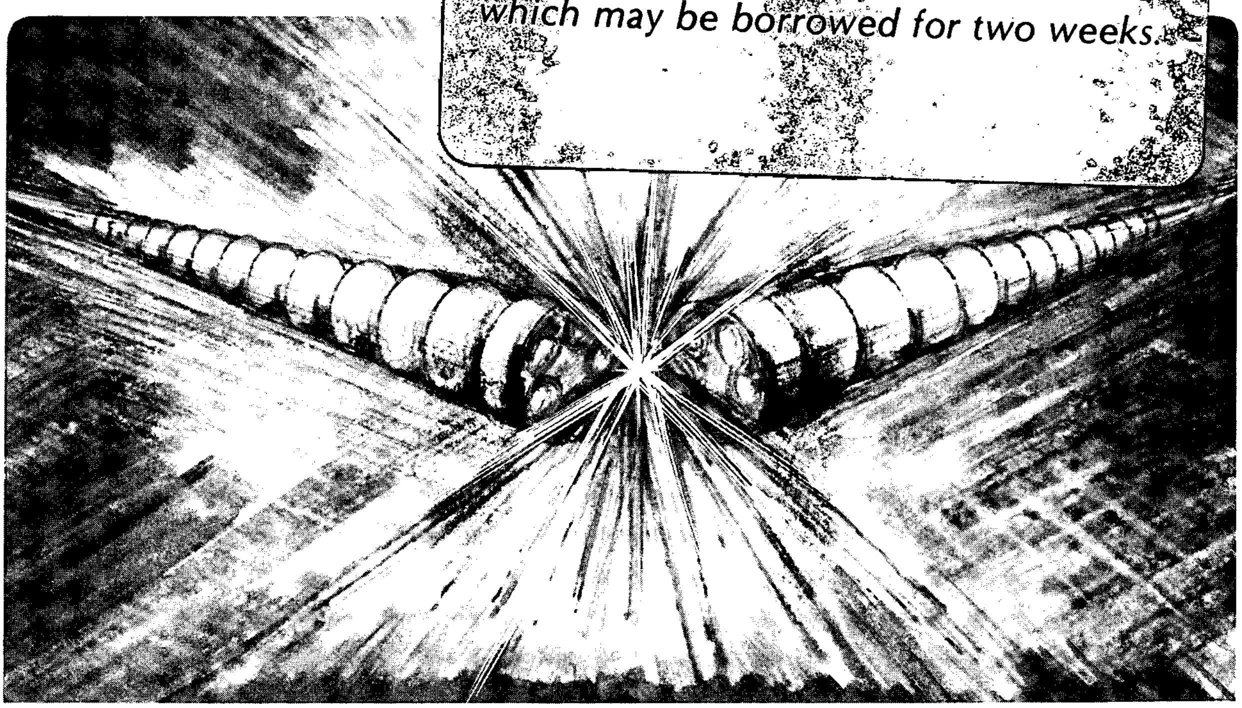

Prepared for the U.S. Department of Energy under Contract DE-AC03-76SF00098

A 1-ampere, 80 keV, Long Pulse H^- Source and Accelerator*

J.W. Kwan, G.D. Ackerman, O.A. Anderson, C.F. Chan, W.S. Cooper,
G.J. deVries, A.F. Lietzke, L. Soroka and W.F. Steele

Lawrence Berkeley Laboratory
University of California
Berkeley, CA 94720

October 21, 1985

Abstract

The design and operation of the surface-conversion H^- ion source and the 80 keV preaccelerator are discussed. Both the source and the preaccelerator, together with the Transverse Field Focussing (TFF) matching and pumping beam transport section (presently being tested), will be parts of a negative-ion-based neutral beam line. Results from testing the source and preaccelerator have shown that the system can accelerate more than 1 amp of H^- ions at 80 keV continuously; the preaccelerator operates at an optimum perveance which matches the one predicted by WOLF code computer simulation. Deconditioning of the preaccelerator due to cesium contamination is a critical problem. A method has been developed to cope with this problem.

* This work was supported by the Director, Office of Energy Research, Office of Fusion Energy, Development & Technology Division of the U.S. Department of Energy under Contract No. DE-AC03-76SF00098.

I. Introduction

In order to produce a neutral beam of more than 150 keV energy with reasonable efficiency, it is necessary to accelerate negative ions rather than positive ions.[1] There are 2 types of negative ion sources being developed at LBL: the surface-conversion type[2,3] and the volume-production type.[4,5] Although the volume-production source may eventually turn out to be a better source in the future, it is not ready to be used in our accelerator study yet. Presently, the surface-conversion source can deliver up to 1.25 amp of H^- ions continuously. The source operation is usually stable and reliable. Nevertheless, the surface-conversion source has one major drawback, which is the usage of cesium in the source. Cesium is known to be undesirable in accelerator systems.

Our present goal is to develop the Transverse Field Focussing (TFF) transport and accelerator system[6] for ribbon-shaped beams to be used in the future negative-ion-based neutral beam line. Fig. 1 shows a conceptual design for a 400 keV, 2 MW/m (of source length) beam line using the TFF accelerator. The TFF system offers several advantages including differential vacuum pumping, beam steering, neutron shielding, and strong focussing abilities.[7] In the TFF system, acceleration of H^- ions will be done in three stages. Starting from the single-slot source, the first stage is a conventional Pierce gun[8] accelerator called the preaccelerator; its function is to inject a uniform, small divergence, ribbon beam into the second stage. The second and the third stages are both TFF sections which transport and accelerate the beam respectively. Only the ion source and the preaccelerator have been constructed and tested as of the time this article was written, hence only they will be discussed here. Further results from testing the remaining TFF sections will be reported later.

II. The Surface-conversion Type Ion Source

The surface-conversion negative ion source at LBL can yield more than 1 ampere of steady H^- ion current.[9] The ion source makes use of the principle that H^- ions can be produced on a metal surface either by desorption[10] or by reflection[11] processes. The formation of H^- ions depends greatly on the surface work function. Since the surface work function can be lowered by adding a small amount (less than a monolayer) of cesium on the surface, H^- production is enhanced by the presence of cesium vapor in the hydrogen discharge. The following sections describe the details in the surface-conversion negative ion source.

II-A. The Source Chamber

Fig. 2 is a cross-sectional view of the source and the preaccelerator. The source chamber is 60 cm tall (in the z direction); the dimensions in the x and y directions are shown in the figure. The device has a translational symmetry along the z axis. For the purpose of plasma confinement, the chamber is surrounded by magnetic cusps of alternating north and south poles. Primary electrons are emitted from the tungsten filaments (the cathode). There are altogether 8 filaments, 4 on each side. They are strategically located at the low magnetic field regions between the cusp lines. The filaments are 1.5 mm in diameter. The chamber wall and the magnet housing together form the source anode, although in this case the effective anode area is actually determined by the width and the strength of the magnet cusps.[12]

II-B. The Converter

The molybdenum converter is located near the center of the source. The converter has a cylindrical surface (12 cm radius); it focuses particles, which are emitted roughly normal to the surface, into the exit aperture. The front surface of the converter has an area of 525 cm^2. In length, the converter is 35 cm tall, which is 10 cm longer than the beam forming slot at the exit aperture. This extra length minimizes effects due to nonuniformity of negative ion production at the converter edges. The converter can be electrically biased to 200 V below the anode potential, or it can be left at the floating potential.

II-C. The Cesium Injection System

Cesium can be injected into the source chamber either from the top or from the bottom of the chamber. The rate of cesium injection is controlled by the oven temperature and by a valve. To avoid cesium condensation, both the valve and the delivery tube must be heated to > 200 ^{o}C. Since the cesium vapor is ionized by the plasma as soon as it comes out of the orifice, the rate of cesium injection does not strictly determine the rate of arrival of cesium ions at the converter surface. Experimentally, it was found that the cesium coverage on the converter surface was a function of many parameters including the injection rate, the converter voltage and the discharge power.

II-D. The Heat Shields

Since any cold surface in the source can pump away useful cesium, heat shields are required for eliminating unnecessary cold surfaces. There are three kinds of heat shields inside the source: the wall liner, the anode liner and the converter shield. All the shields have poor thermal contact to the water-cooled parts of the source chamber, therefore they become hot in the discharge due to radiation. Experimentally, we have found that there are two advantages in running the source with the hot liners. First, the cesium consumption rate was reduced, and second, the source remained clean at all times.

The anode liner can serve an additional purpose apart from cutting down on the cesium pumping. By adjusting the gap between the liner and the magnet, we can vary the strength of the magnet cusps which in turn determines the effective anode area. Too little anode area can cause the plasma to "mode-flip" (see section III-C) whereas too much anode area allows extra loss of plasma electrons. The converter shield, which is electrically floating, also has a second purpose: it prevents the plasma ions from reaching the backside of the converter electrode. Only the front surface of the converter is exposed to the plasma for negative ion production. The presence of the converter shield reduces the converter current drain by a factor of 3 (from 60 amp to 20 amp). This reduction of the converter current can be very significant when it comes to controlling electrical "spotting" (unipolar arcing, also see section III-C) on the converter.

II-E. Control of Leakage Electrons

It is very important in a negative ion source to minimize the amount of leakage electrons going into the accelerator because both the electrons and the negative ions are accelerated together. The leakage electrons are useless in producing neutral beam, but they can increase the power loss and the heat load in the system. In our source the suppression of leakage electrons is done by two different means. First, the magnet cusps provide a magnetic filter across the exit aperture. This magnetic filtering is just strong enough to reflect the light electrons, yet it is weak enough to let the heavy negative ions to get through with only a small offset in the ion trajectory. Second, the aperture collimator is electrically insulated from the anode such that, according to Ehlers and Leung,[13] applying a positive potential bias on the collimator can electrostatically suppress the leakage of electrons from the source.

III. Source Operation

III-A. Discharge Characteristics

The surface-conversion source is always operated in the emission-limited region of the I-V curve for the purpose of getting longer filament life and better arc stability. In this region, the arc current is independently controlled by the filament heater current. Consequently, the arc voltage can be adjusted without affecting the arc current (due to the large dynamic impedance). Source operation is in dc mode. It generally takes about 15 minutes for the source to reach equilibrium temperature after initial start-up. Typical numbers for the arc voltage and currents are -100 V and 100 A respectively. Other typical parameters can be found in Table 1. All voltages indicated in the table were measured with respect to the anode potential.

The converter behaves like a large probe in the plasma; it collects an ion current which scales with the arc power. At -130 V converter voltage, the converter current can be as much as 25 A. At zero converter current, the floating potential of the converter is approximately -30 V. The electron temperature is estimated to be several eV. Measurements of positive ion saturation current density using a Langmuir probe have found $J_i \approx 60$ mA/cm^2. The plasma density (n_i) is found to be $\approx 2\times10^{11}$ cm^{-3} according to the expression for J_i:

$$J_i = n_i e \times 0.6\,(kT_e/m_i)^{1/2} \quad ,$$

where k is the Boltzmann constant, T_e is the electron temperature, and m_i is the average positive ion mass.

III-B. H^- Production

Under normal conditions, our surface-conversion source can produce up to 1.25 amp of H^- continuously. The corresponding current density is 10 mA/cm^2 at the source aperture exit. Other than the total beam current, the steadiness and the uniformity of the current density are also important factors determining the usefulness of a source.

H^- production in a surface-conversion source depends on the amount of cesium coverage on the converter surface and the flux of positive ions on the surface. The cesium coverage is controlled by both the converter bias voltage and the injection rate of cesium neutrals into the source. The converter voltage also determines the velocity of positive ions arriving at the converter surface, i.e. the sputtering rate. In addition, the positive ion flux is a function of the plasma density (hence the arc power). Thus in order to produce a certain level of steady H^- current, it is necessary to find a matching condition for the arc power, the converter voltage, and the cesium injection rate. Interestingly, the matching condition is also the condition which gives the best uniformity in the beam current density. This is a fortunate coincidence because there is no independent parameter in the source to control the beam uniformity. In our experiment, we have found that the H^- output is low if the cesium injection rate is either too high or too low. This phenomenon suggests that at each combination of arc power level and converter voltage, there is an optimum cesium coverage which gives the maximum H^- yield, as illustrated in Fig. 3.

If the converter voltage is suddenly dropped from -100 V to the floating potential or to the anode potential, then there will be a corresponding sudden change in the rate of cesium sputtering off the converter surface. Consequently, when -100 V is applied to the converter again, and provided that the cesium injection rate remains steady during this time interval, the amount of cesium coverage on the converter surface would be higher than before. By simply turning the converter voltage off, waiting for a brief moment (about a second or so), and then turning the voltage back on, we can increase the cesium coverage on the converter surface.[14] If the converter is below optimum cesium coverage beforehand, turning the converter power off and on will cause the H^- output to increase. In contrast, if the converter is above optimum coverage, the same action will cause the H^- output to drop. At optimum cesium coverage, the change in the H^- output due to this action is minimum. Experimentally, this simple converter test indicates when the optimum cesium coverage occurrs during a matching condition in which the arc, the converter voltage, the cesium injection rate, and the H^- output are all in steady states. The converter test therefore provides a way to quickly check for matching conditons without being necessary to wait for a long time in order to reach a steady state. Fig. 4 shows the typical responses of the H^- output during the converter test for the cases of under-optimum, over-optimum, and optimum cesium coverage.

III-C. Instability Control

A steady H^- current from the source can be maintained for hours of operation provided there is no disruption in the discharge. Nevertheless, in the past we have experienced two problems which can lead to discharge disruption: "spotting" and "mode flipping". They are discussed in the remaining part of this section.

Arc spotting is a common problem in a discharge using filament emission. It happens when some surface at negative potential with respect to the plasma other than the filament emits electrons. Spotting can dissipate a lot of arc power without producing any useful plasma. Once a spot has started, the only way to extinguish it is to briefly interrupt the arc power supply current. Detectors which sense the presence of a "spot" by measuring the over-current were installed to protect the source. We have seen spotting occur on both the arc and the converter surfaces. Spotting can also happen on an isolated conducting surface at floating potential; marks of spotting which look like "chicken tracks" were also observed on the electrically isolated metal converter shield.

Spotting tends to occur when a source is dirty or when the arc voltage is too high. In spotting, vaporized insulator material may condense at some undesirable location, such as the anode surface. For example, boron nitride was found to be a bad insulator material from this point of view when used at places where spotting can possibly occur.

A magnetic multipole ion source can be operated in two different stable modes depending on the discharge voltage, the gas pressure and the available anode area.[15,16] These two modes are characterized by their arc impedances: one is low, and the other is high. The low impedance mode is also called the efficient mode because in this mode the arc power supply can readily deliver power for producing higher plasma density. It is possible for the source to switch spontaneously from the efficient mode to the inefficient mode under certain conditions; this is referred to as "mode-flipping". Generally, we want to keep the source running in the efficient mode. In the remaining part of this section we shall briefly discuss the cause of mode-flipping and the ways to avoid it.

In an ion source there are four potentials to be considered. They are the anode potential, the cathode potential, the plasma potential, and the floating potential. For convenience, we can choose the anode potential to be a reference (e.g. the anode can be the ground point); all other voltages are measured with respect to the anode. The cathode potential (or the discharge potential) is fixed by the arc power supply voltage; it determines the primary electron energy. The plasma adjusts its plasma potential spontaneously in order to balance the flow of charged particles at the cathode and the anode. The floating potential is always negative with respect to the plasma potential; the potential difference depends mostly on the electron temperature. As shown in Fig. 5, the plasma potential can be either positive or negative (i.e. above or below the anode potential). For the positive case, the plasma electrons experience a retarding potential at the electron-rich anode sheath, which results in a better electron confinement for the source. Better electron confinement leads to higher plasma density, making this the efficient mode. In this mode, the plasma potential is usually a few volts above anode. The charged particle current density at the anode is space-charge limited, whereas the discharge current at the cathode is emission limited. For a fixed effective anode area, as the discharge current increases, the plasma potential will decrease accordingly in order to reduce the electron retardation. This relation continues to hold until the plasma potential becomes equal to the anode potential. Further reduction of plasma potential below the anode potential is not possible without incurring a drastic change in the discharge. As the plasma potential approaches the anode potential, the discharge becomes unstable and it can spontaneously transform ("mode-flip") into another stable mode. In this new mode, the plasma potential is negative with respect to the anode hence the anode sheath is ion-rich. Since the anode sheath is no longer retarding electrons, the electron confinement is poor. The plasma density drops drastically with a big increase in the arc impedance. The arc current in this inefficient mode can be a few times smaller than the arc current in the efficient mode, although the arc voltage may or may not be kept constant depending on the particular power supply in use. In the inefficient mode, both the cathode emission and the anode current are space charge limited.

To avoid mode-flipping, the discharge voltage and the gas pressure must be kept above certain levels. Raising either the arc voltage or the gas pressure has the effect of increasing the plasma density which in turns keeps the plasma potential above the anode potential. Since it is not desirable to run the source at high arc voltage and high gas pressure (high voltage is bad for spotting and high pressure is bad for gas efficiency), an alternate way is to increase anode area. We can conveniently adjust the effective anode area in our ion source by using the anode liner, as was described in section II-D.

IV. The 80 keV Preaccelerator

The preaccelerator has the geometry of a conventional Pierce type accelerator. It consists of four electrodes, which we have named as the beam-forming electrode, the gradient electrode, the suppressor, and the ground electrode. A drawing which shows the position of the preaccelerator in relation to the source can be found in Fig. 2. Once again, like the ion source, the preaccelerator has a translational symmetry along the z-axis.

Each electrode has an opening, in the shape of a rectangular slot, for the beam to pass through. The slots are made long enough such that their ends do not interfere with the beam edges as defined by the exit aperture piece in the ion source.

A schematic circuit diagram of the preaccelerator electrodes is depicted in Fig. 6. As shown in the diagram, only one high voltage power supply is used to drive a resistive voltage divider. The voltage ratios between the four electrodes can be easily determined according to the resistance values of the divider resistors. There are pros and cons in using a voltage divider to provide the different electrode voltages as opposed to using separate power supplies. One advantage is that it is more economical. Secondly, the synchronization of turning on all the high voltages is implicit in the case of a divider. On the other hand, the regulation of the various voltages is difficult when there is a significant amount of current flowing to or from the electrodes. The voltage divider is never as convenient as a separate power supply when it comes to changing voltage ratios between the electrodes.

Designing of the entire beam line, from the preaccelerator to the TFF accelerator, was done with the aid of a 2-dimensional ion optics code called WOLF.[17] Typical results of the self-consistent (including space charge effect) electrical equipotentials and ion trajectories from WOLF are shown in Fig. 7a and 7b. Using WOLF, it is possible to predict the optimum perveance of the preaccelerator. The WOLF code predictions will be compared with experimental results from the emittance measurement later in section VI.

V. The Preaccelerator Operation

V-A. General Descriptions

Holding high voltage on the electrodes is a key issue to the operation of an electrostatic accelerator. Prior to any source and preaccelerator operation, all the parts that are required to hold high voltages are tested ("hi-potted") to their corresponding high voltage levels. This process is generally referred to as conditioning. Hi-potting, which can be done with a dc hi-potter, conditions the electrodes to hold high voltage in vacuum. Hi-potting is also valuable in looking for assembly errors which can lead to breakdown before beam operation.

The second issue in the operation of an electrostatic accelerator is beam optics. A good ion beam ought to be stable, uniform and have low beam divergence. In order to achieve these criteria, the source must supply a steady beam with uniform ion current density at the beam forming electrode. Self-extraction of the H^- ions is achieved by focussing the converter surface at the exit aperture. The current density and the velocity distribution of the H^- ion beam at the aperture are primarily determined by the conditions of the converter and the discharge plasma. In particular, once the source is set to produce a certain amount of H^- beam, just changing the accelerating voltage would not affect the total beam current at all. For this reason, in tuning for the optimum perveance the accelerating voltage is adjusted while the beam current is kept constant (positive ion accelerator tuning is usually done in the opposite way).

Applying the high voltage to the resistive divider is done by closing an SCR switch. The electrodes are protected from being damaged due to arc breakdown by a power supply crowbar circuit which diverts the breakdown current and allows the SCR switch to open. Breakdowns are indicated by a rapid drop in the applied high voltages, or a sudden increase in the currents. Level detectors are used to monitor these signals and a positive identification of a breakdown will trigger the power supply crowbar circuit.

The energy stored in the stray capacitance of the source (to ground) could cause damaging peak currents to flow when breakdowns occur, therefore a transiently dissipative "snubber", see Fig. 6, has been installed in the circuit to limit this current to a few hundred amperes,[18] which is a sufficiently low current that electrodes are not damaged.

V-B. Deconditioning and Reconditioning of Accelerator Electrodes

In order to produce a steady beam, the source must be running in steady state before turning on the accelerator. However, as stated earlier in section III-A, the source takes some time to reach equilibrium from a cold start. During this time the cesium vapor, which is required to run the surface-conversion source, can escape through the source aperture into the preaccelerator. Cesium deposited on the accelerator electrodes degrades the high voltage holding capability of the preaccelerator gaps. The result is that the preaccelerator, which had been conditioned to hold high voltage before starting up the source, is already deconditioned due to cesium contamination by the time the source is running steadily. Applying high voltage to the preaccelerator at this time, either with or without the source running, would cause a breakdown to occur at the gap between the gradient electrode and the suppressor (this gap has the highest electric field gradient in the system, see Fig. 7a). The cesium contamination is accumulative: the longer we run the source, the lower the breakdown threshold will become.

Perhaps the most important phenomenon we found was that the preaccelerator which was deconditioned by cesium contamination could be reconditioned by applying high voltage to the electrodes. This finding actually shed some light on the viability of using a surface-conversion type ion source in accelerator systems. To keep the accelerator functioning, it is essential to avoid the contamination from building up. This is done by applying pulses of high voltage to the accelerator electrodes starting from the first minute when the source is being turned on.

Breakdown usually occurs at the gradient electrode. The condition of the preaccelerator can be monitored by reading the current at the gradient electrode during the application of high voltage to the electrodes. A large current to this electrode would indicate that it is close to a breakdown situation. Fig. 8 shows the effect of reconditioning with a high voltage pulse applied to the preaccelerator. The gradient electrode current drops almost exponentially to a finite limit during the pulse length. If no more high voltage pulse is applied to the preaccelerator for some time, the gradient electrode current will become very large at the initial moment of the next applied high voltage pulse. The size of the initial gradient electrode current increases with the amplitude of the high voltage pulse, with the rate of cesium injection in running the source, and with the amount of time between applied pulses.

V-C. Present Results

Once the the source and the preaccelerator have been conditioned, the preaccelerator can be tuned to the proper perveance by adjusting the voltage to match the negative ion current. At the correct perveance, we have produced up to 1 ampere of H^- ions at 80 keV energy steadily for as long as 30 seconds (see Fig. 9). The limit of 30 seconds on the pulse length is a restriction imposed by heating of the resistive divider. With an improved power supply system, the preaccelerator can be run in the dc mode since all other critical parts in the system are water cooled.

VI. Beam Diagnostics

VI-A. Emittance Measurement

The most important objectives in our testing were to find out the proper perveance of the preaccelerator and the corresponding beam divergence. This was done by measuring the beam emittance downstream from the preaccelerator. The beam emittance contains information from which the beam divergence can be determined. A schematic diagram of the emittance probe[19] is shown in Fig. 10. It consists of a pair of parallel deflection plates, an entrance slit, an exit slit, and a Faraday charge collector. The device was mounted so that it could be translated along two axes perpendicular to the beam, and was located 10 cm downstream from the preaccelerator.

The angular distribution of the beam current, at a fixed position, was determined by varying the potential difference across the deflection plates and measuring the collected current. This measurement was repeated at 20 different positions as the probe was moved across the beam in the direction of the narrow dimension of the beam. By combining the data in the 20 scans, an emittance diagram such as the one shown in Fig. 11 could be constructed.

Emittance diagrams are probably the best way to describe the "quality" of particle beams. The emittance diagram shown in Fig. 11 is a typical example of a divergent beam as indicated by the relatively large range of angle extended across the pattern, and more importantly, by the tilting of the pattern's axis of symmetry. In comparison, the emittance diagram shown in Fig. 12a represents a beam of smaller divergence (≈ 2 degrees). The values of accelerating voltage and beam current in producing a beam of minimum divergence define the best perveance of the preaccelerator ($p=I/V^{3/2}$). We found that the best perveance occurred at $p=4.2\times10^{-8}$ amp/$V^{3/2}$ independent of the accelerating voltage. The corresponding emittance containing 90% of the beam was found to be 107 cm-mrad.

It is interesting to compare the measured emittance diagram (Fig. 12a) with the one generated by WOLF code as in Fig. 12b. Apart from the small fraction of beam at the extreme angle, the two diagrams agree quite well. In addition, both the simulation and the measurement agreed on the same value of best perveance.

VI-B. Electron Impurity Measurement

The amount of electrons contained in the ion beam was measured by a magnetic analyser. The device is schematically shown in Fig. 13. The permanent magnets provide a magnetic field of the order of 700 Gauss. The electrons are separated from the ions such that they will be collected by 2 different carbon cups. The assembly is enclosed in a steel case in order to minimize the leakage stray magnetic field. The analyser and the emittance probe were both mounted on the same transporter except that the emittance probe entrance slit was located at the center of the transporter whereas the magnetic analyser aperture was offset 3 cm to one side (the closest we could fit them together). Due to this offset, the magnetic analyser could only see one-half of the beam as limited by the maximum travel of the transporter.

A typical result obtained from the analyser is shown in Fig. 14. Integrating the electron density and the ion density across the mid-plane of the beam, one finds that the electron current is approximately 10-12 percent of the total beam current. This amount is not sufficient to affect the results from the emittance measurement. Interestingly, the electron distribution is not identical to that of the ions: there is an extra peak at 3.5 cm away from the center. It is possible that the electrons in the extra peak have a different origin than those electrons in the central peak. While the latter probably originated from the converter, the former may be secondary electrons generated in the preaccelerator region, or leakage electrons from the source plasma, both of which will have different trajectories from the negative ions.

Another interesting phenomenon was that the electron content varies with the perveance, as indicated in Fig. 15. The perveance which produced the minimum electron content in the beam happened to coincide with the best perveance found in the emittance measurement. This can be explained in the following manner. The electrons in the beam, or at least part of the electrons in the beam, were secondary electrons produced by the stray negative ions in the preaccelerator. At best perveance, the amount of such ions intercepted on electrodes was at minimum, consequently, the electron content in the beam was also at minimum.

VII. Conclusion

The testing of the surface-conversion negative ion source and the preaccelerator for the Transverse Field Focussing accelerator has been very successful. The source ran steadily, producing up to 1.25 A of H^- ions continuously. The preaccelerator accelerated 1 A of beam at 80kV for 30 seconds. Only approximately 10 to 15 percent of the beam current was found to be electrons. Deconditioning of the accelerator electrodes by cesium contamination was found to be a critical problem. However, a method was developed to recondition the electrodes while the source is operating. Beam diagnostic measurements have shown the emittance to be in good agreement with the computer simulation.

VIII. Acknowledgements

We would like to thank D. Deutscher, D. Kippenhan and D. Williams for assistance in experimental work. The technical work of J.A. Paterson, L.A. Biagi, H.H. Hughes, H.M. Owren, and members of their groups are gratefully acknowledged. We would also like to thank Prof. Wulf Kunkel for his valuable comment on the manuscript. This work is supported by the U.S. Department of Energy, Office of Fusion Energy, under Contract No. DE-AC03-76SF00098.

References

1. W.S. Cooper, Nuclear Technology / Fusion, 4, p632 (1983).
2. K.W. Ehlers and K.N. Leung, Rev. Sci. Instrum., 51, p721 (1980).
3. K.N. Leung and K.W. Ehlers, Rev. Sci. Instrum., 53, p803 (1982).
4. K.N. Leung, K.W. Ehlers and M. Bacal, Rev. Sci. Instrum., 54, p56 (1983).
5. R.L. York, R.R. Stevens, Jr., K.N. Leung and K.W. Ehlers, Rev. Sci. Instrum., 55, p681 (1984).
6. O.A. Anderson, Proceedings of the 3rd International Symposium on the Production and Neutralization of Negative Ions and Beams (Brookhaven, New York), p473 (1983).
7. W.S. Cooper, Proceedings of the 3rd International Symposium on the Production and Neutralization of Negative Ions and Beams (Brookhaven, New York), p605 (1983).
8. J.R. Pierce, "Theory and Design of Electron Beams", 2nd ed., D. Van Nostrand Co., Inc., New York (1954).
9. A.F. Lietzke, K.W. Ehlers and K.N. Leung, Proceedings of the 3rd International Symposium on the Production and Neutralization of Negative Ions and Beams (Brookhaven, New York), p344 (1983).
10. M.L. Yu, Phys. Rev. Lett., 40, p574 (1978).
11. J.R. Hiskes, A. Karo and M. Gardner, J. Appl. Phys., 47, p3888 (1976).
12. A.J.T. Holmes, Rev. Sci. Instrum., 52, p1874 (1981).
13. K.W. Ehlers and K.N. Leung, Appl. Phys. Lett., 38, p287 (1981).
14. K.W. Ehlers and K.N. Leung, Proceedings of the 3rd International Symposium on the Production and Neutralization of Negative Ions and Beams (Brookhaven, New York), p227 (1983).
15. A.P.H. Goede and T.S. Green, Phys. Fluids, 25, p1797 (1982).

16. D. M. Goebel, Phys. Fluids, 25, p1093 (1982).

17. W.S. Cooper, K. Halbach and S.B. Magyary, Proceedings of the 2nd Symposium on Ion Sources and Formation of Ion Beams, Berkeley, California, (1974).

18. H.M. Owren, W.R. Baker, K.H. Berkner, D.B. Hopkins, and D.J. Massoletti, Proceedings of the 12th Symposium on Fusion Technology, Julich, W. Germany, (1982).

19. P.W. Allison, J.D. Sherman, and D. B. Holtkamp, Particle Accelerator Conference, Santa Fe, New Mexico (1983).

Figure Captions

Fig. 1 A conceptual design for a 400 keV, 2 MW/m (of source length) beam line.

Fig. 2 The surface-conversion negative ion source and the preaccelerator. X direction is along the beam line, y direction is towards top of the page, and z direction is coming out of the paper.

Fig. 3 Production of H^- ions as a function of the cesium coverage on the converter surface.

Fig. 4 Typical responses of H^- output during the converter cesium coverage test (a. converter voltage pulse shape, b. under-optimum case, c. over-optimum case, d. optimum case).

Fig. 5 Relation of the anode potential, the cathode potential, the plasma potential and the floating potential in the source.

Fig. 6 A schematic circuit diagram of the preaccelerator electrodes.

Fig. 7a Electrical equipotentials, including space-charge effects, obtained from the WOLF code.

Fig. 7b Ion trajectories obtained from WOLF code calculation. (The space charge effect is neglected in the source plasma and in the extraction sheath regions, whereas in the preaccelerator region the Poisson-Vlasov equation is solved self-consistently including space charge effect).

Fig. 8 The effect of preaccelerator electrode reconditioning by a high voltage pulse.

Fig. 9 An oscillogram record of the 80.5 keV (upper trace), 1 A (lower trace) H^- beam with a pulse length of 30.3 seconds.

Fig. 10 A schematic diagram of the emittance probe.

Fig. 11 A typical example of an emittance diagram showing a divergent beam. The percentage labeled at each contour indicates the fraction of the total beam current enclosed by that contour.

Fig. 12a The emittance diagram measured from an ion beam at optimum perveance (minimum beam divergence).

Fig. 12b The emittance diagram of an optimum perveance beam according to WOLF code calculation.

Fig. 13 A schematic diagram of the magnetic analyser.

Fig. 14 A typical result obtained from the magnetic analyser.

Fig. 15 The electron content in the beam as a function of perveance.

Table 1

Typical Parameters of the Surface-conversion Source

H_2 gas flow rate	2 Torr-liter/sec
Source filling pressure	1.5 mTorr
Gas efficiency	4.5 percent
Arc voltage	-100 V
Arc current	100 A
Total filament current	760 A
Filament life time	> 300 hrs.
Converter voltage	-130 V
Converter current	25 A
Cesium oven temperature	260 ^{o}C
Cesium valve opening rate	2 sec/15 sec (ON/OFF)
Cesium consumption rate	0.1 gm/hr.-amp
H^- ion beam output	> 1 A
H^- ion current density at entrance to accelerator	> 10 ma/cm^2
Electron content in ion beam	12 percent
H^- ion temperature	5 eV
Beam divergence	2 degrees

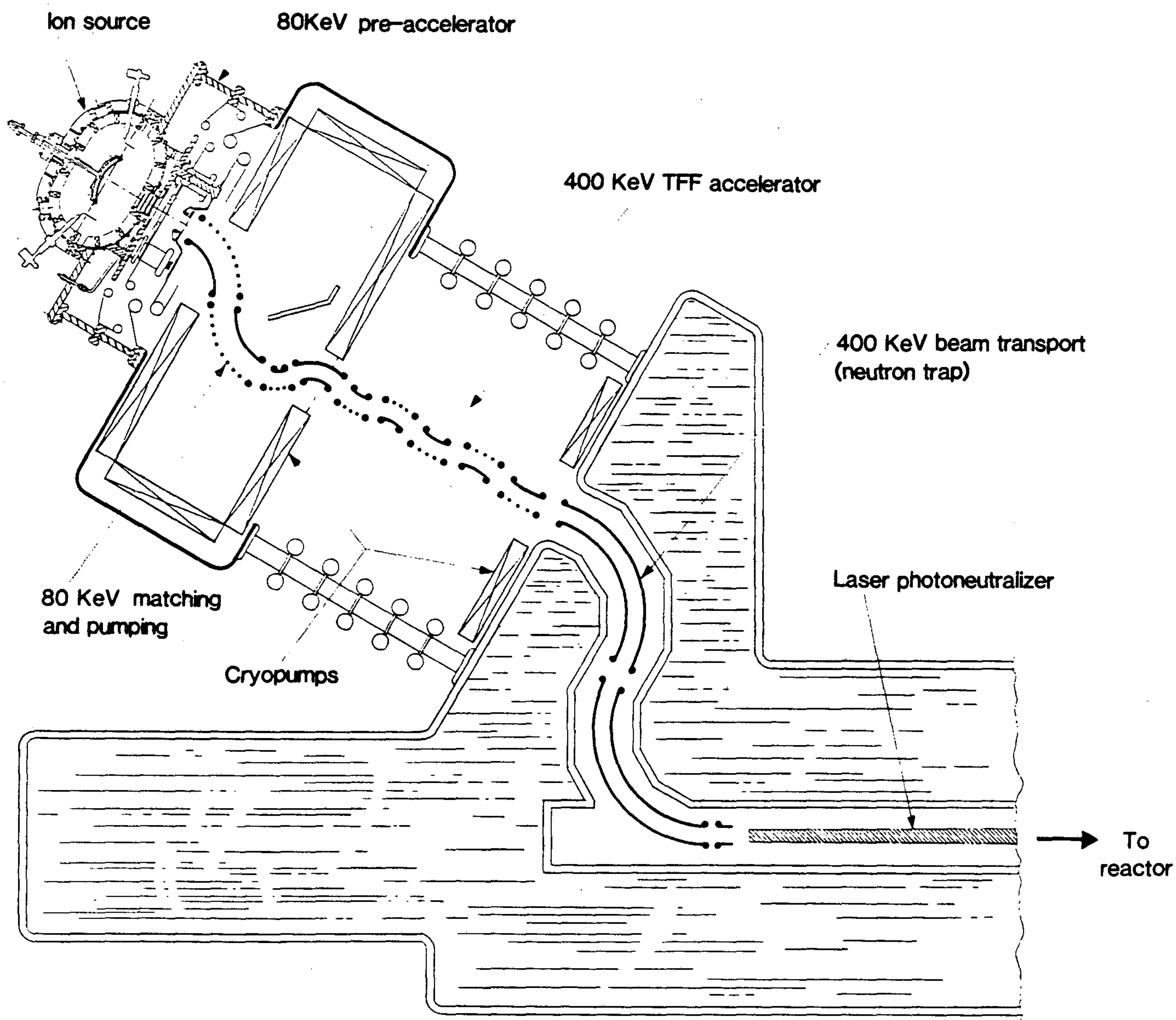

XBL 8310-12264

Fig. 1

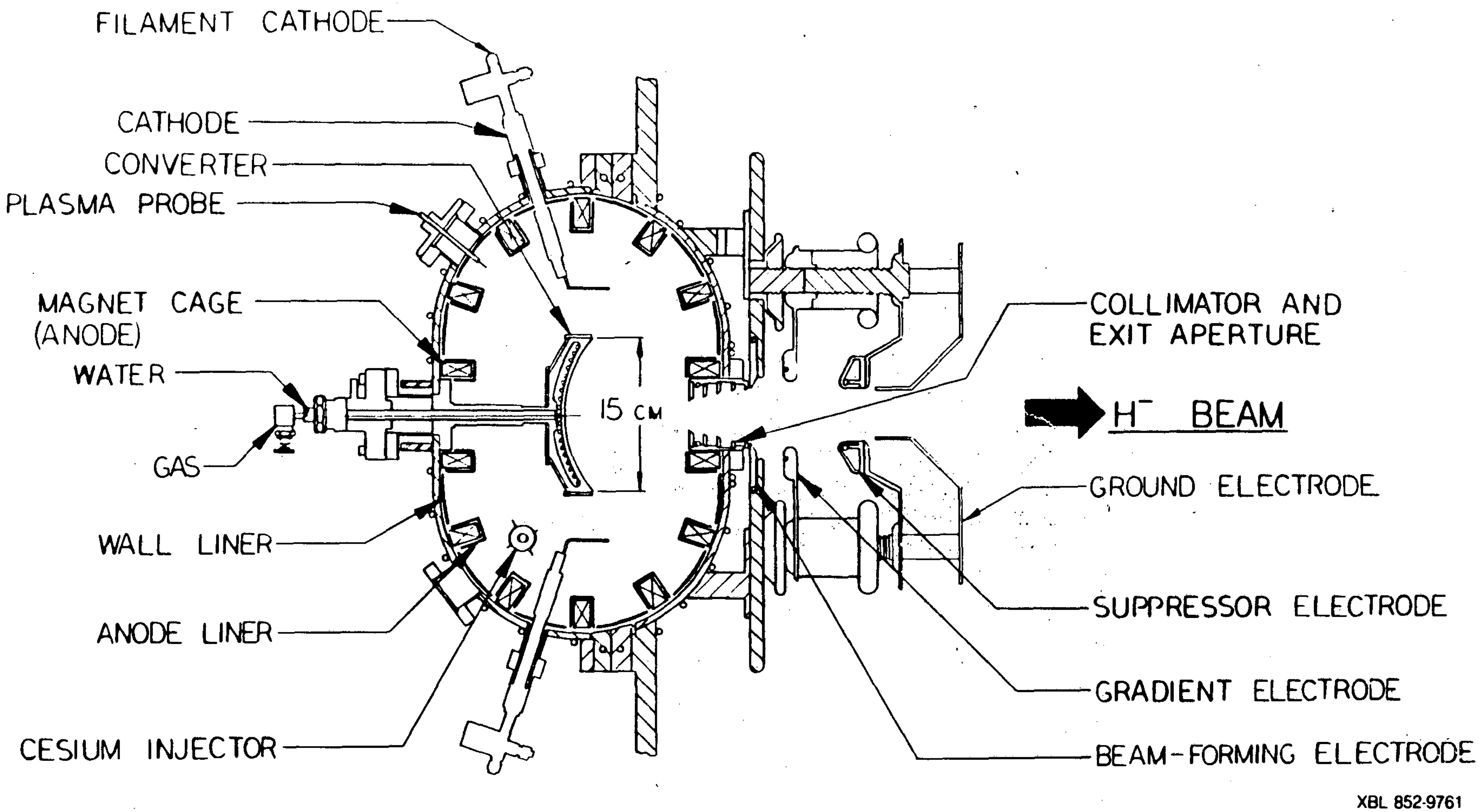
FILAMENT CATHODE
CATHODE
CONVERTER
PLASMA PROBE
MAGNET CAGE
(ANODE)
WATER
GAS
WALL LINER
ANODE LINER
CESIUM INJECTOR
15 CM
COLLIMATOR AND
EXIT APERTURE
H⁻ BEAM
GROUND ELECTRODE
SUPPRESSOR ELECTRODE
GRADIENT ELECTRODE
BEAM-FORMING ELECTRODE
XBL 852-9761

Fig. 2

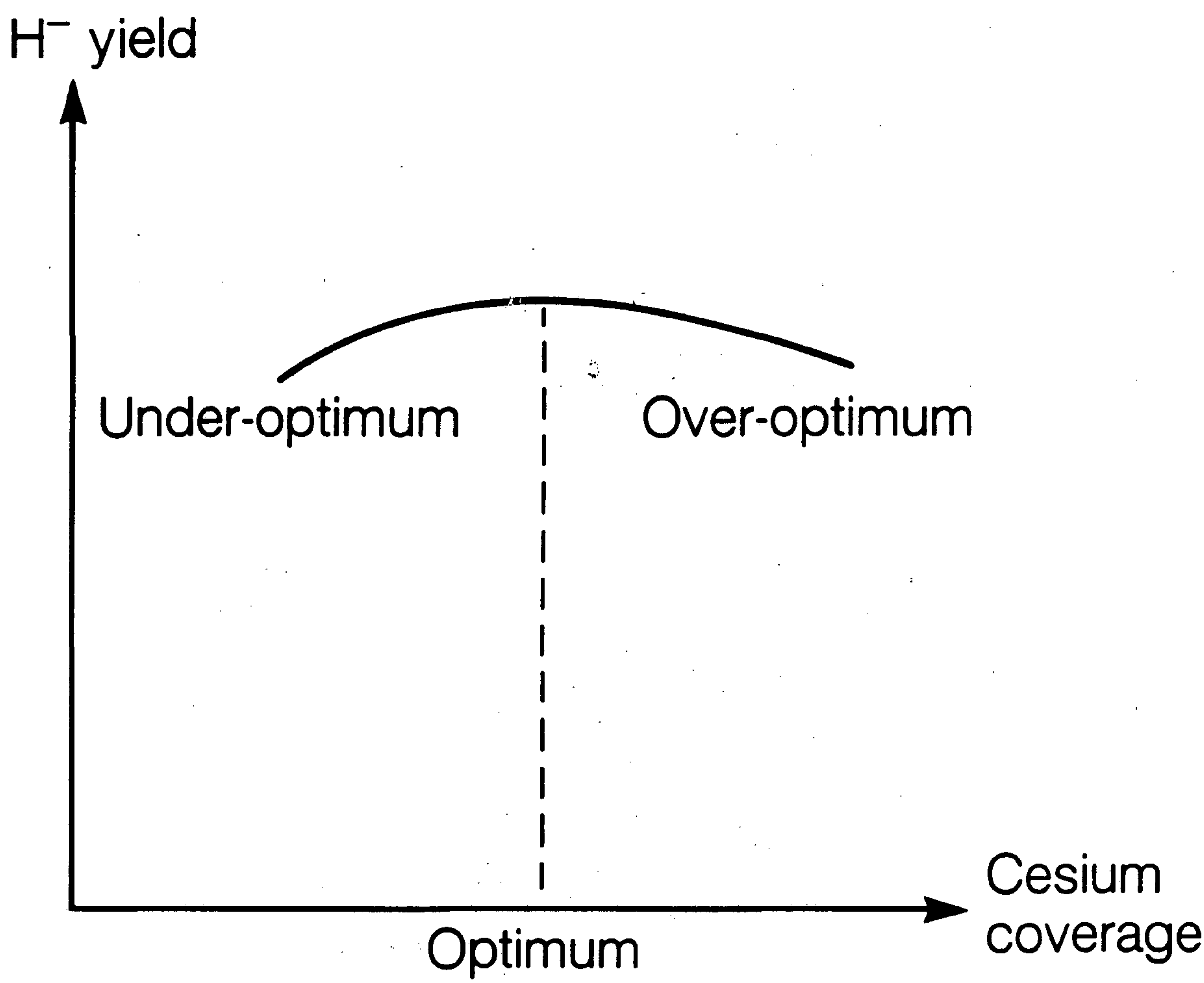

XBL 852-9759

Fig. 3

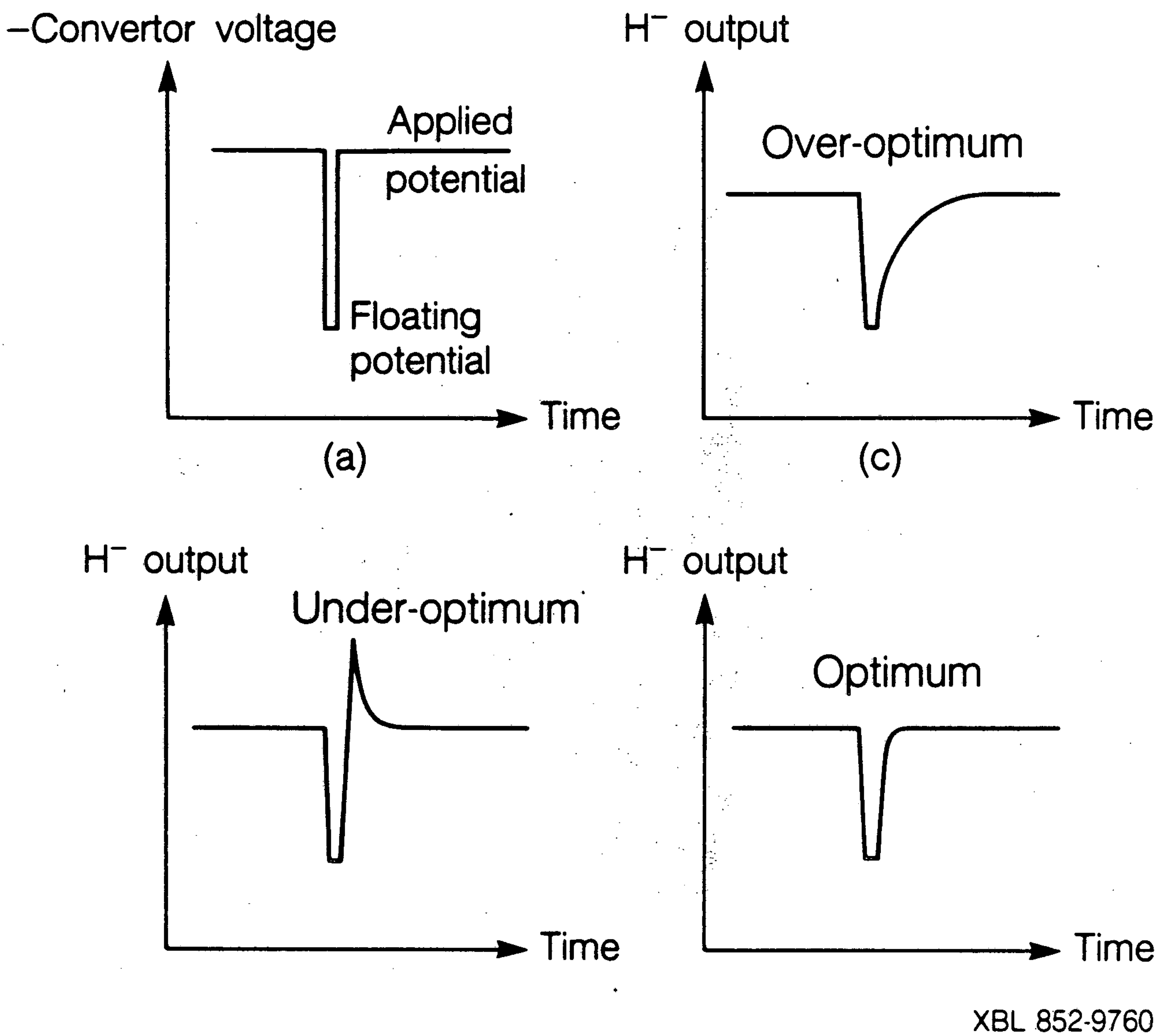

−Convertor voltage
Applied
potential
Floating
potential
Time
(a)
H⁻ output
Over-optimum
Time
(c)
H⁻ output
Under-optimum
Time
H⁻ output
Optimum
Time
XBL 852-9760

Fig. 4

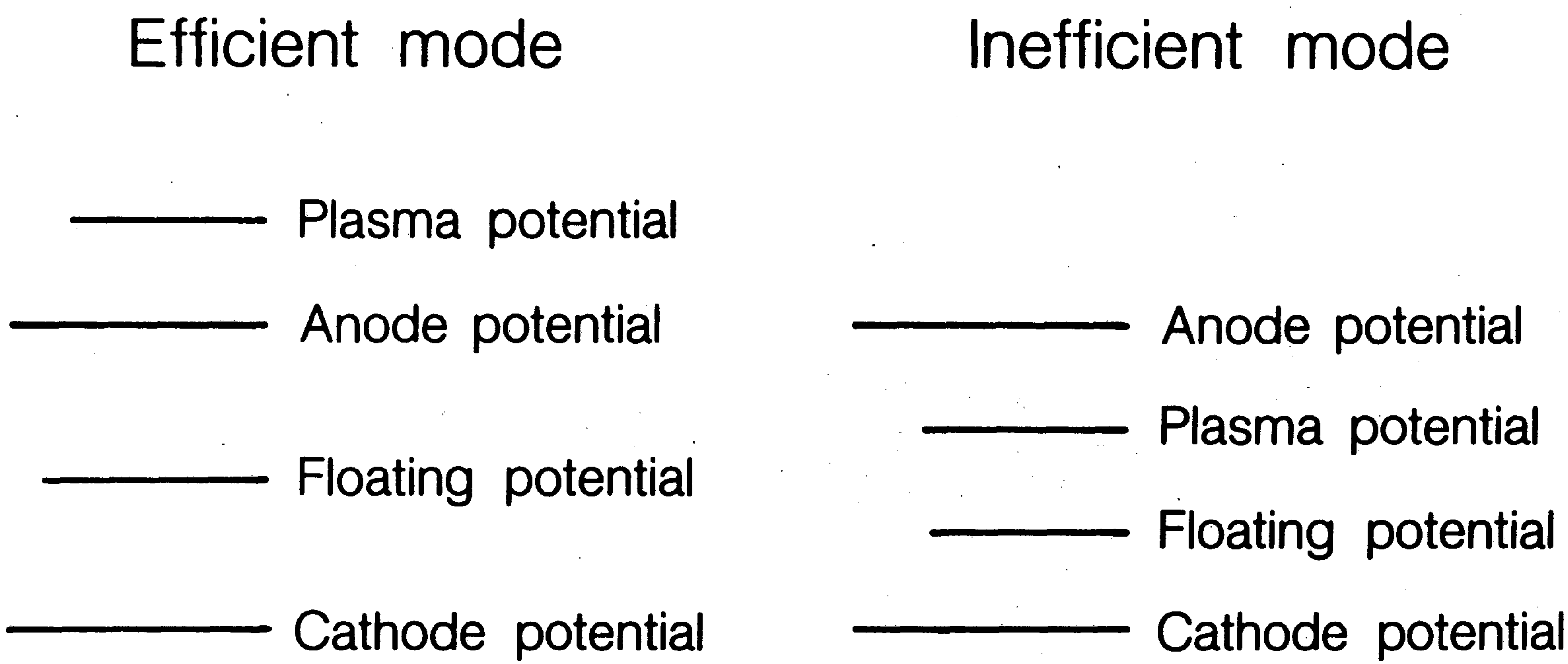
Efficient mode
Plasma potential
Anode potential
Floating potential
Cathode potential
Inefficient mode
Anode potential
Plasma potential
Floating potential
Cathode potential

Fig. 5

Electrical circuit diagram of the source and the preaccelerator

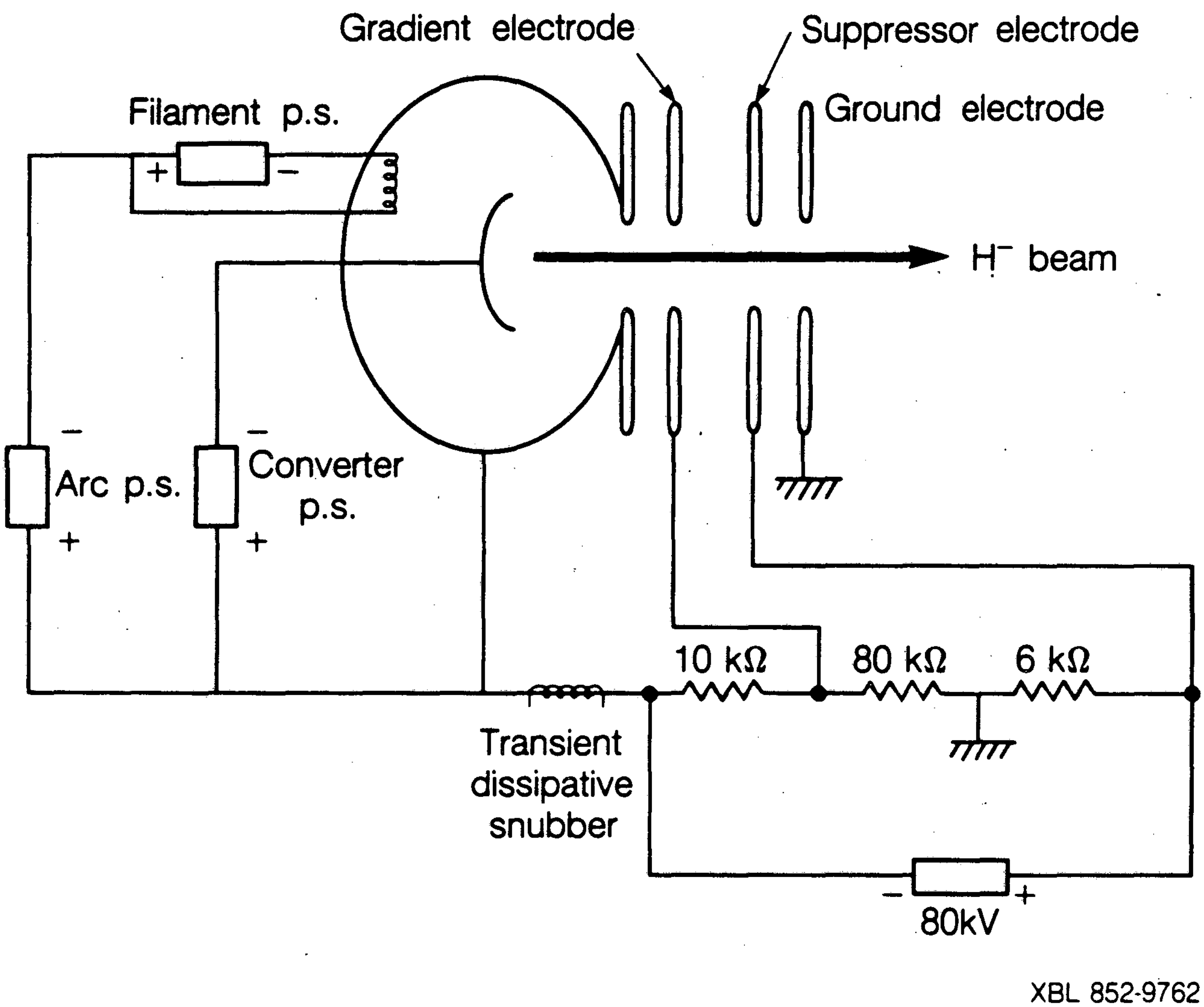

Fig. 6

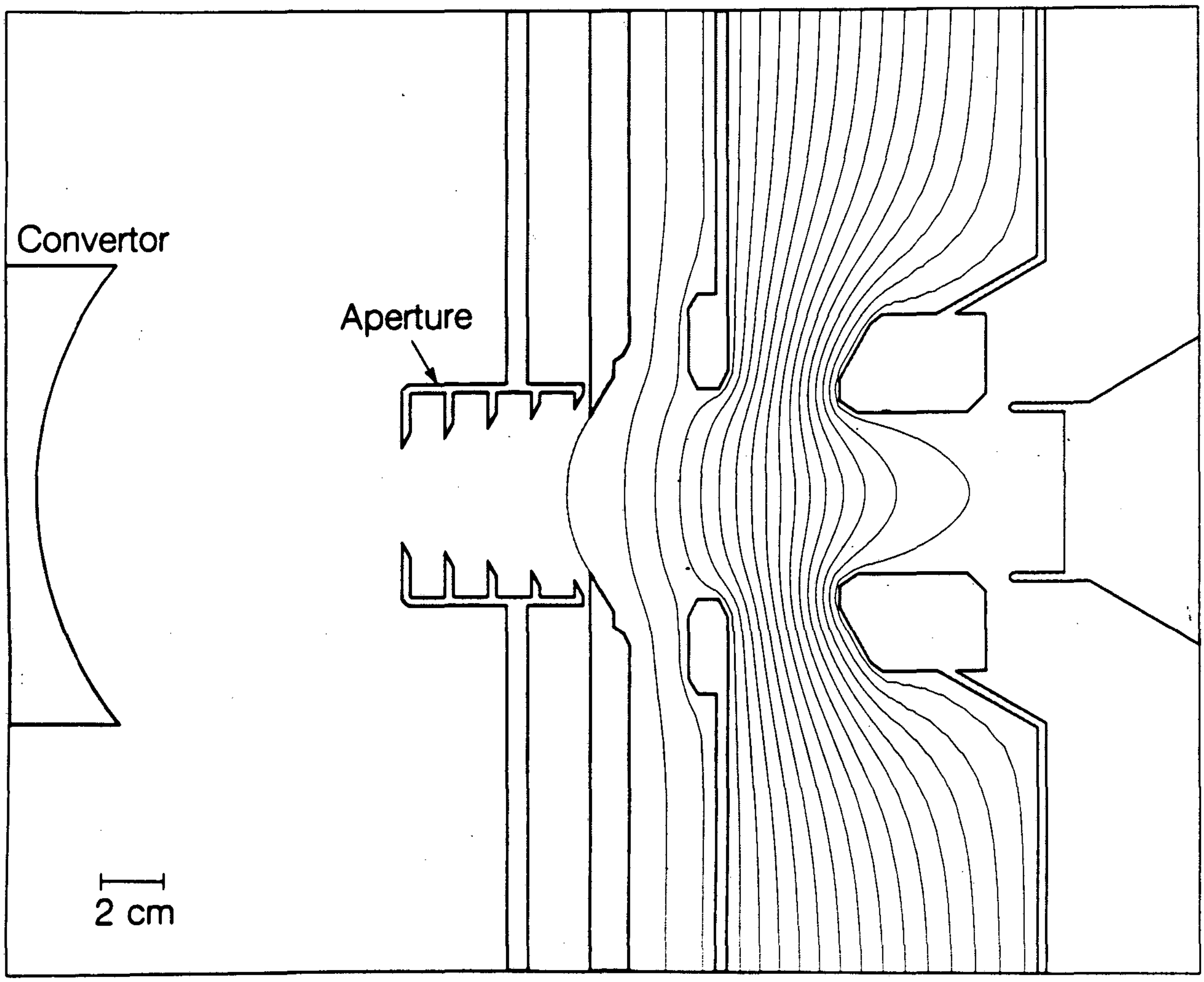

Fig. 7a

Acceleration of ion beam as computed by WOLF Code
(82.5kV / 0.92 Amp)

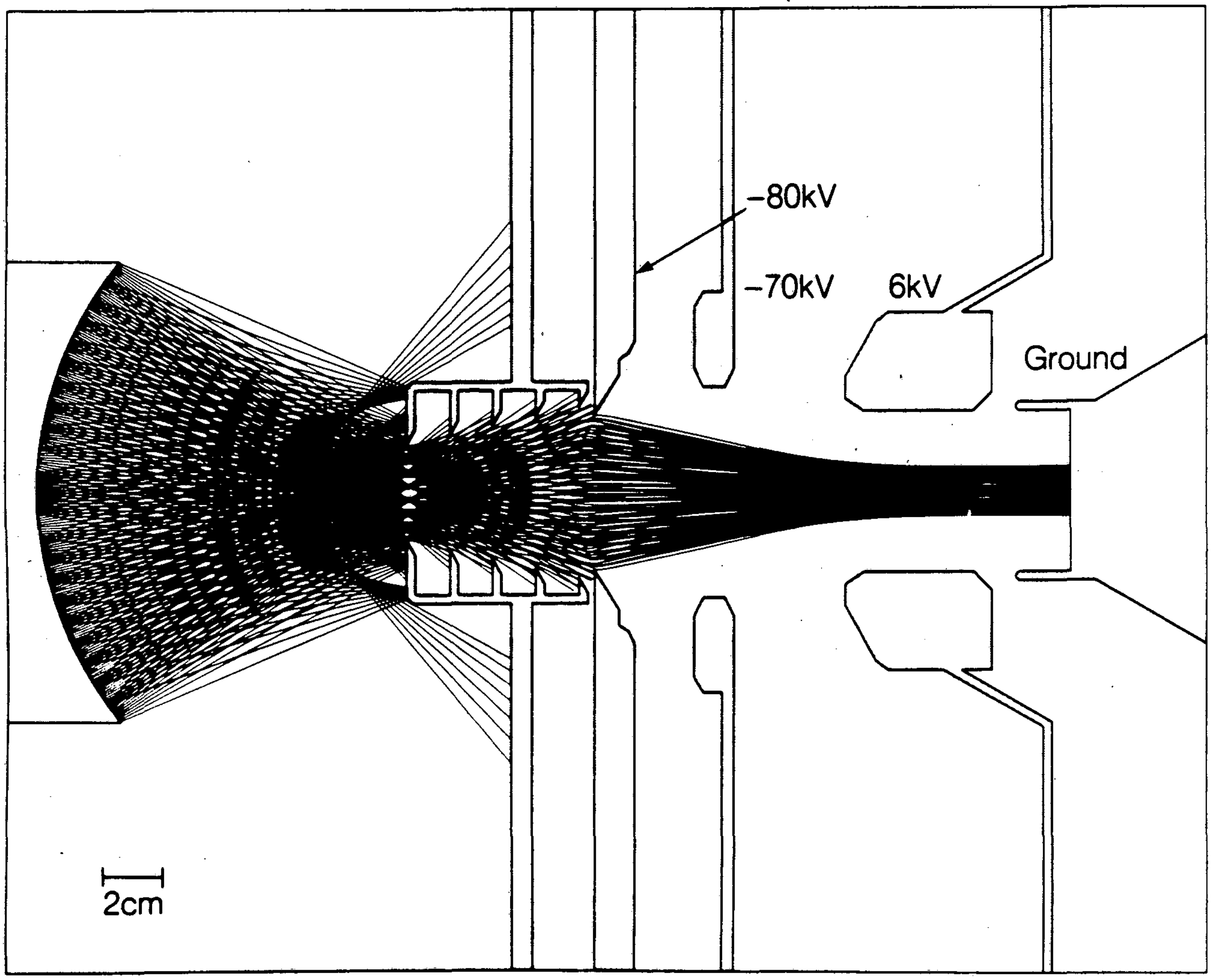

XBL 852-9769

Fig. 7b

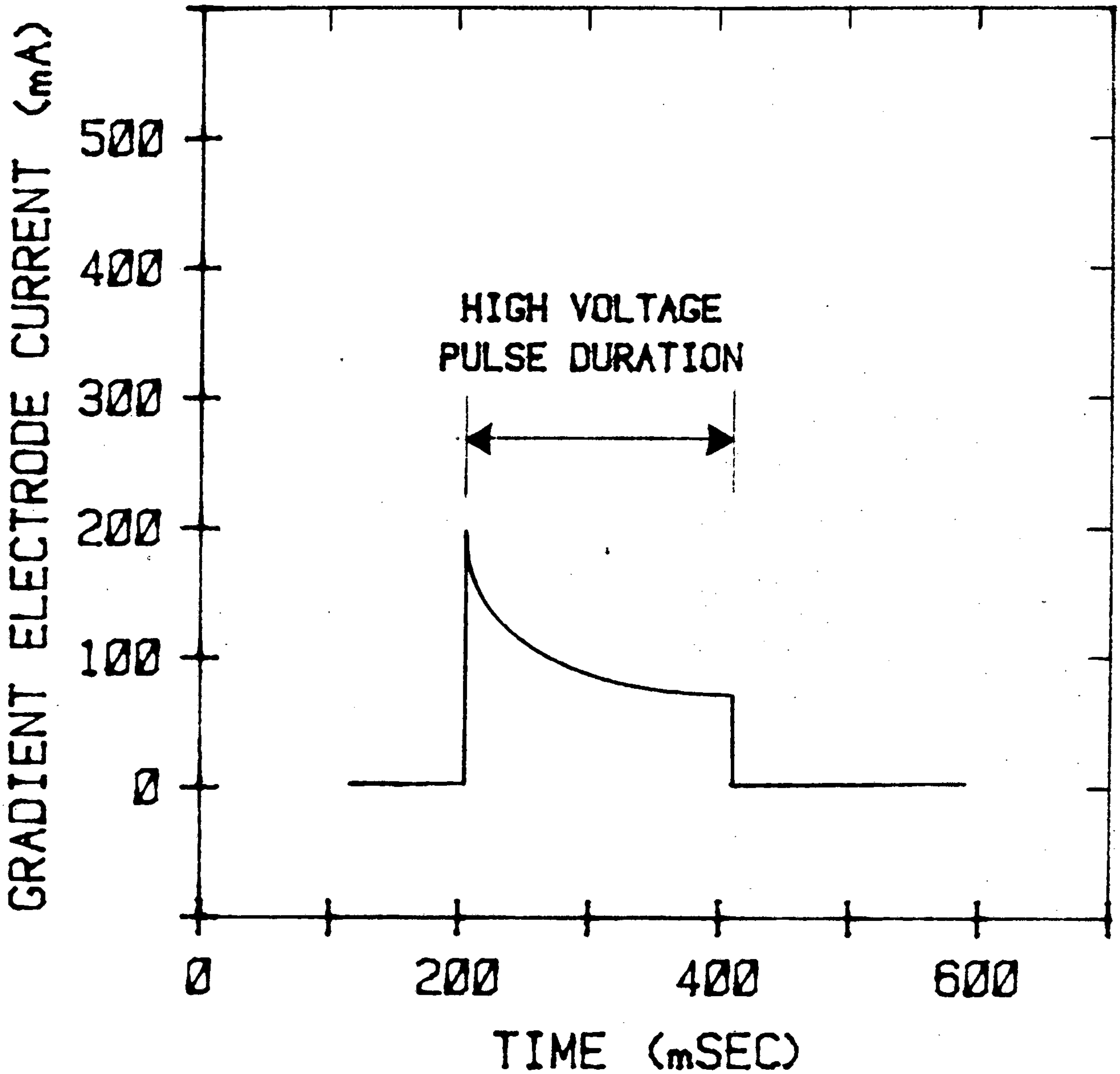

XBL 859-3812

Fig. 8

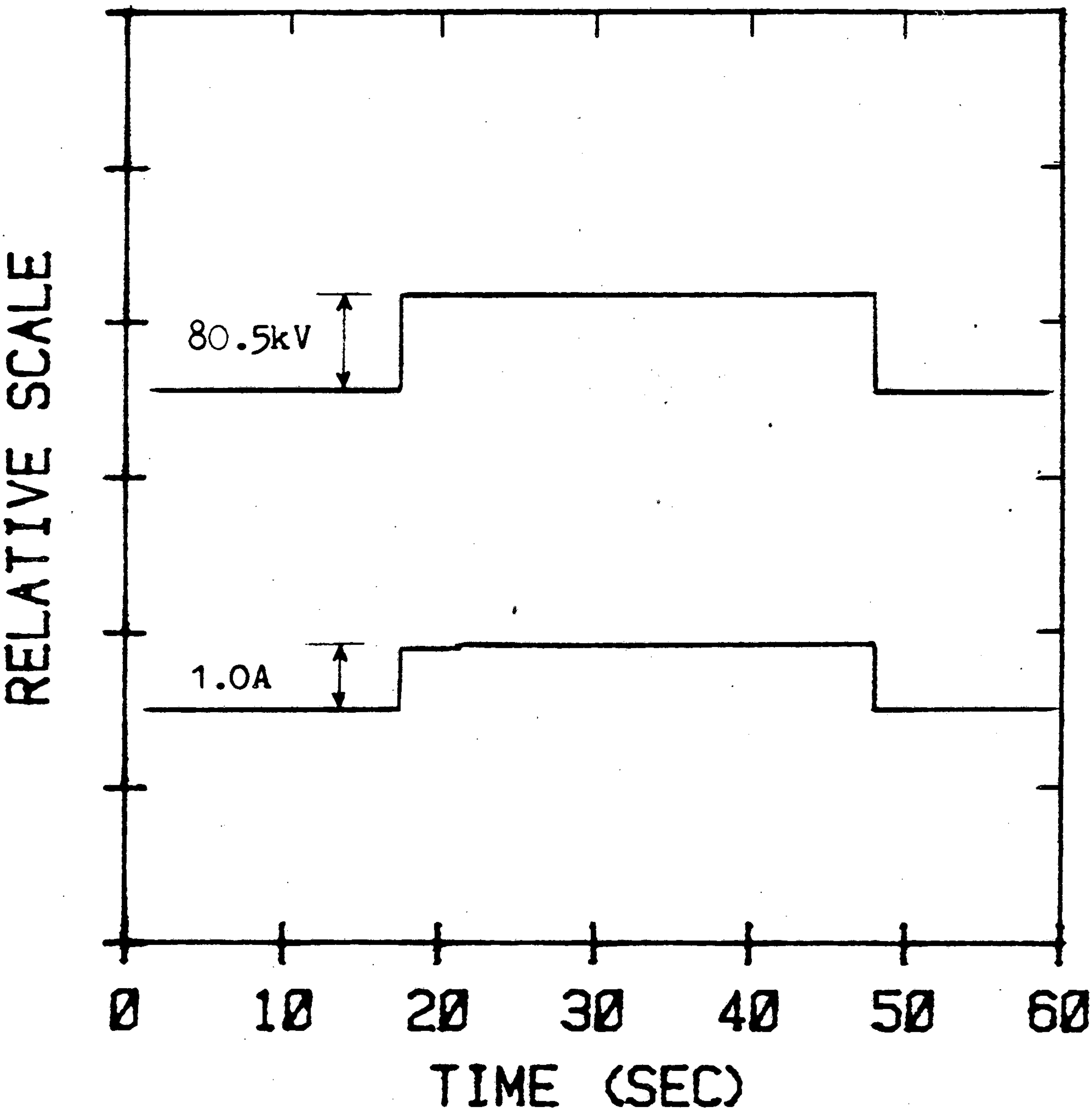

XBL 859-3811

Fig. 9

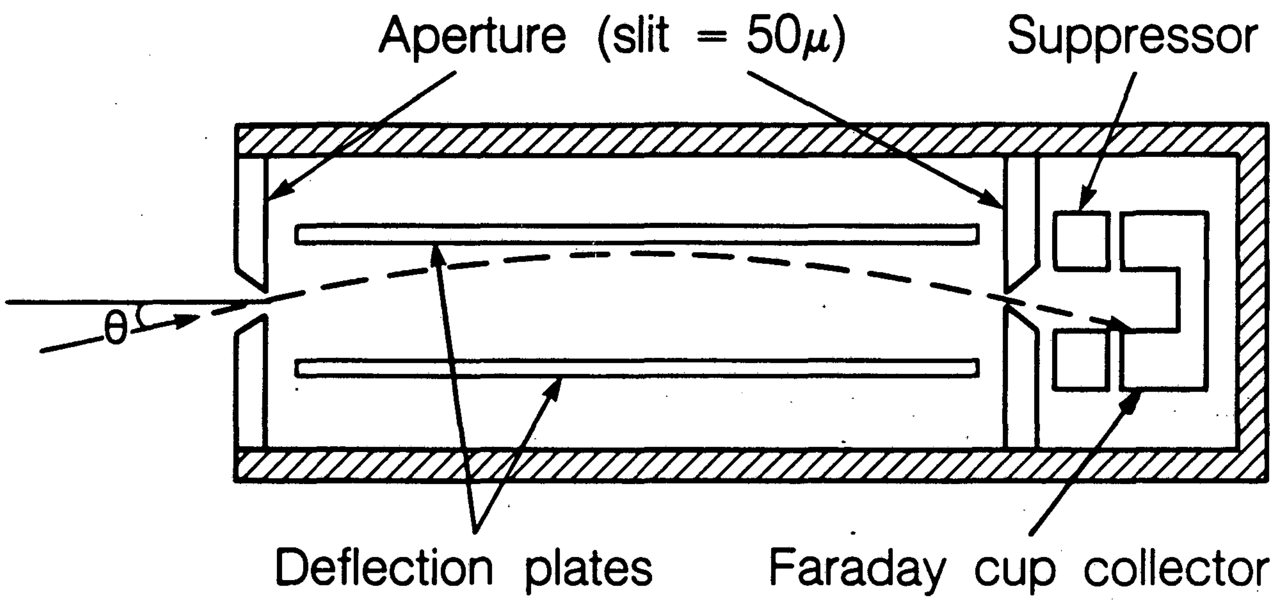

Range: ± 76mrad
Resolution: 0.4mrad
Deflection plate voltage: ±500V (scanning)
Suppressor voltage: −100V

XBL 852-9765

Fig. 10

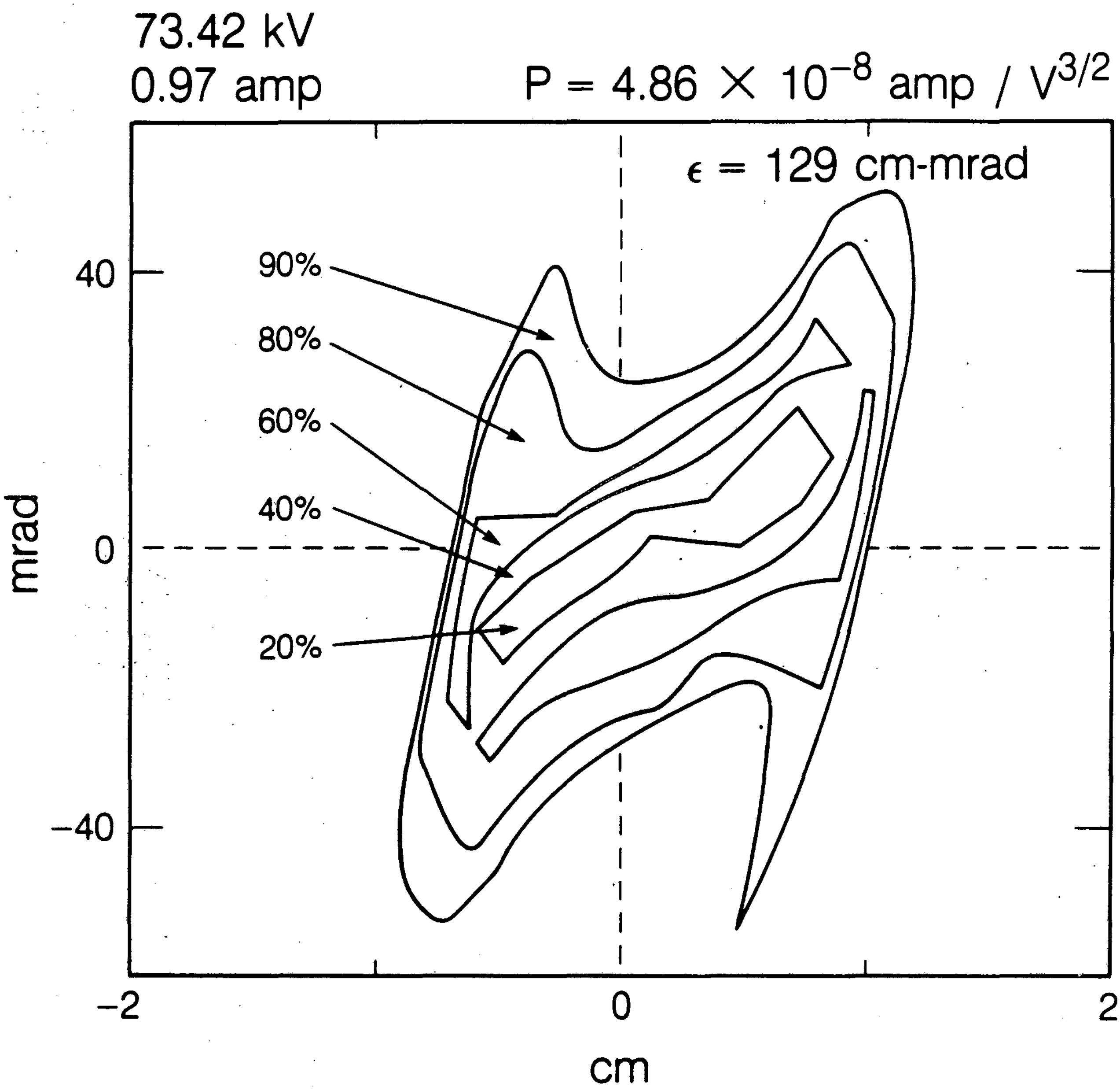
73.42 kV
0.97 amp
P = 4.86 × 10−8 amp / V3/2
ε = 129 cm-mrad
90%
80%
60%
40%
20%
40
0
−40
mrad
−2
0
2
cm
XBL 852-9766

Fig. 11

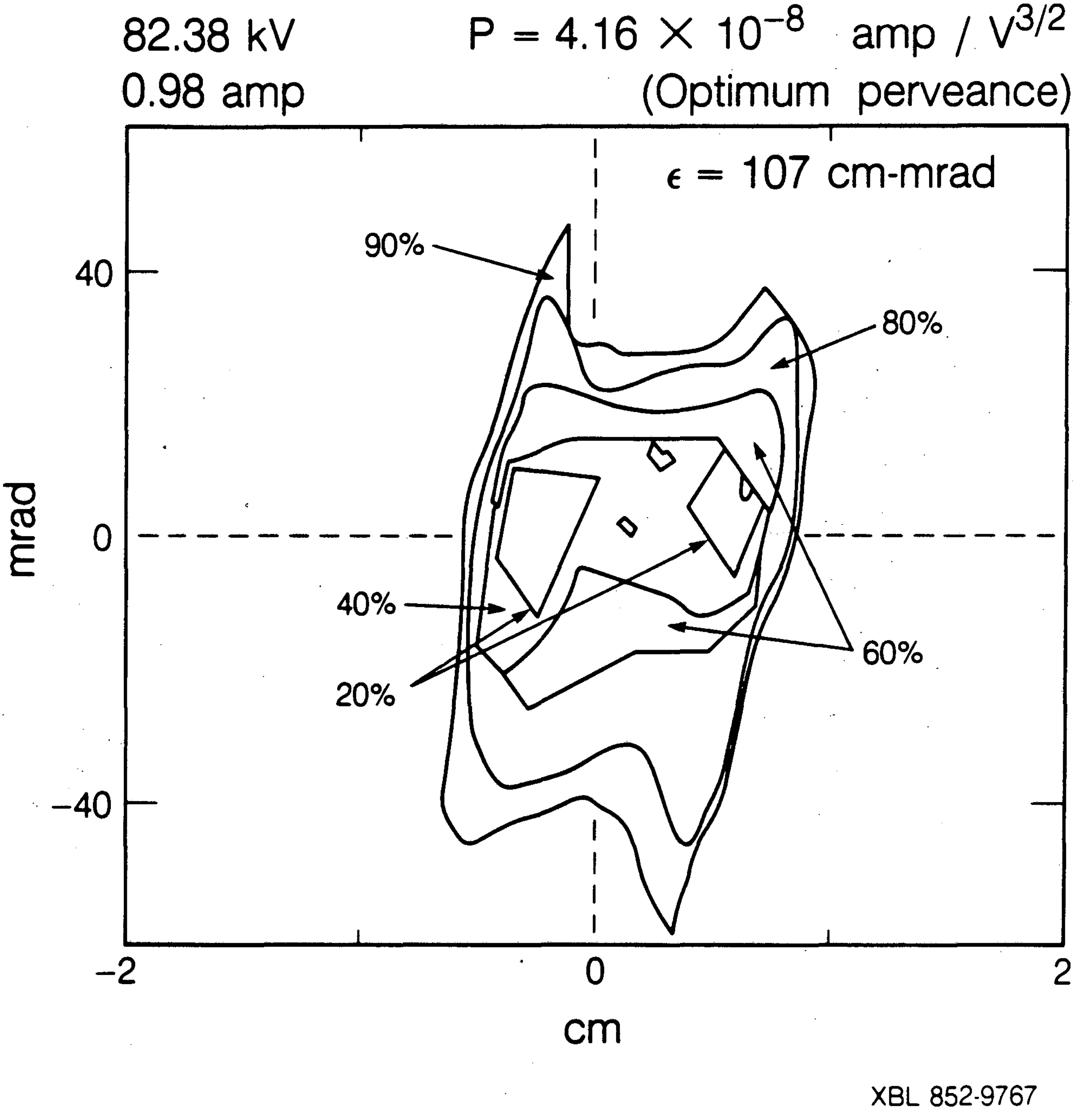
82.38 kV
0.98 amp
P = 4.16 × 10^{-8} amp / V$^{3/2}$
(Optimum perveance)
ϵ = 107 cm-mrad
90%
80%
60%
40%
20%
40
0
−40
mrad
−2
0
2
cm
XBL 852-9767

Fig. 12a

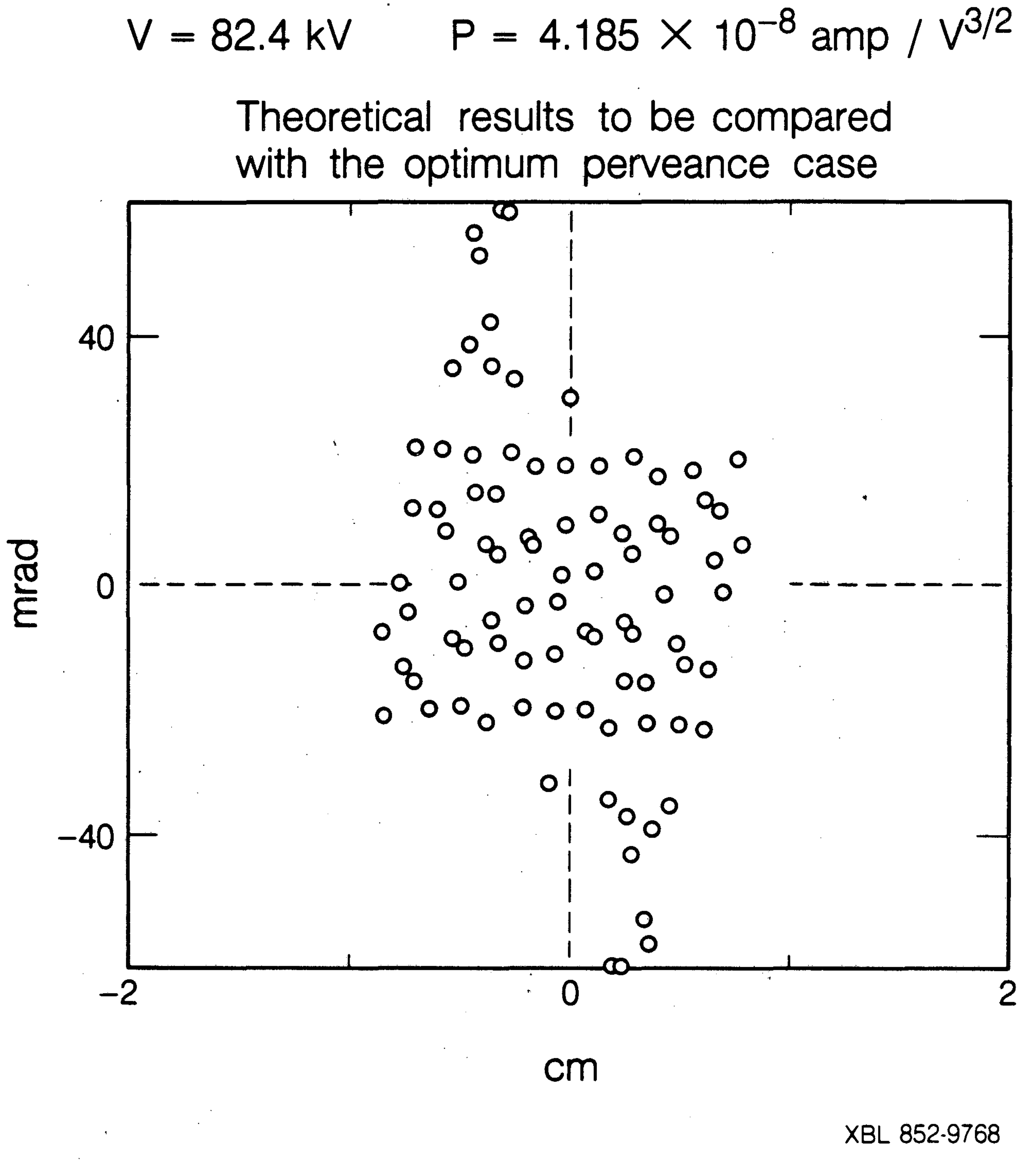

V = 82.4 kV P = 4.185 × 10^-8 amp / V^3/2
Theoretical results to be compared
with the optimum perveance case
40
0
-40
mrad
-2
0
2
cm
XBL 852-9768

Fig. 12b

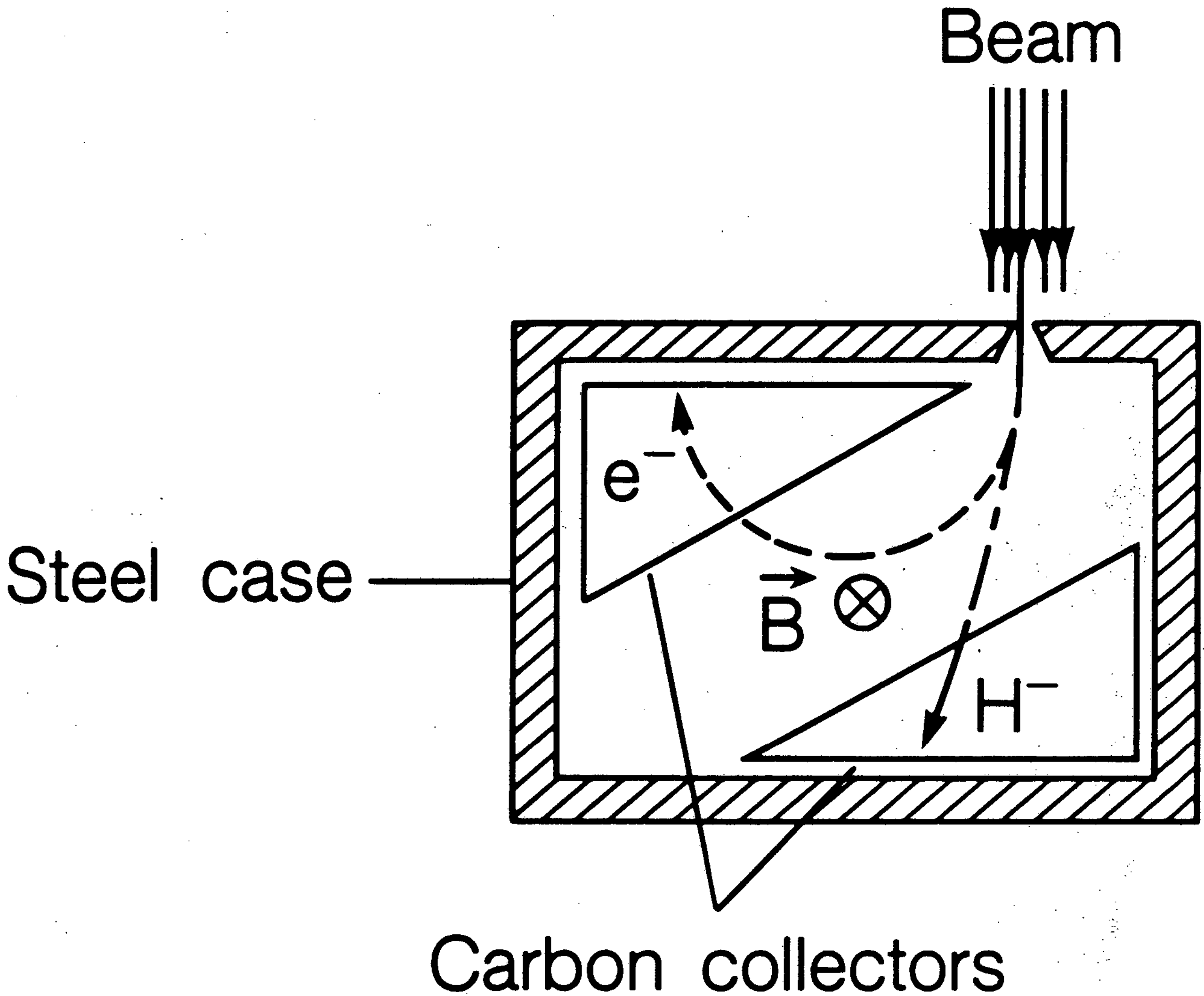

XBL 859 3814

Fig. 13

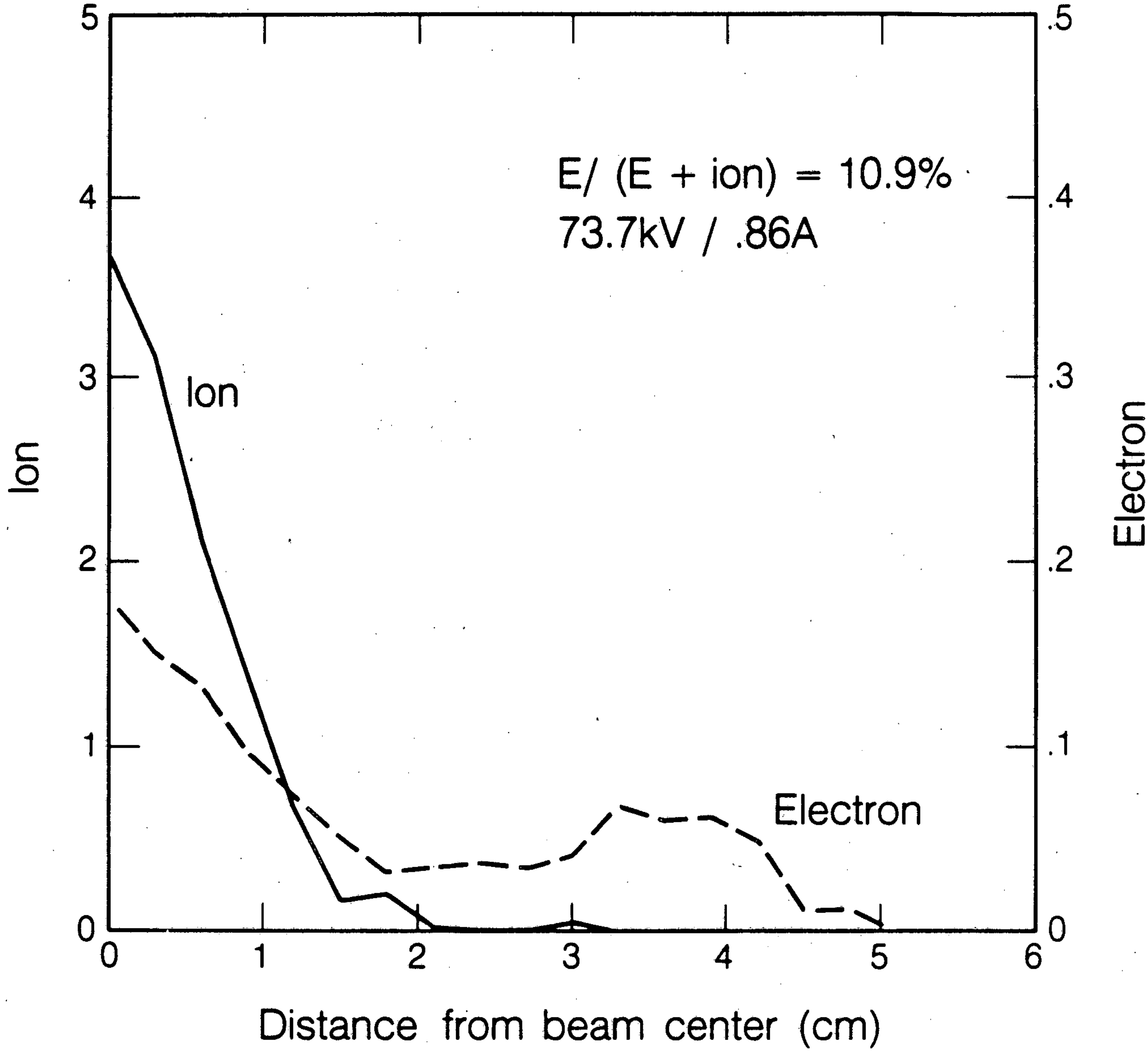

XBL 859-3815

Fig. 14

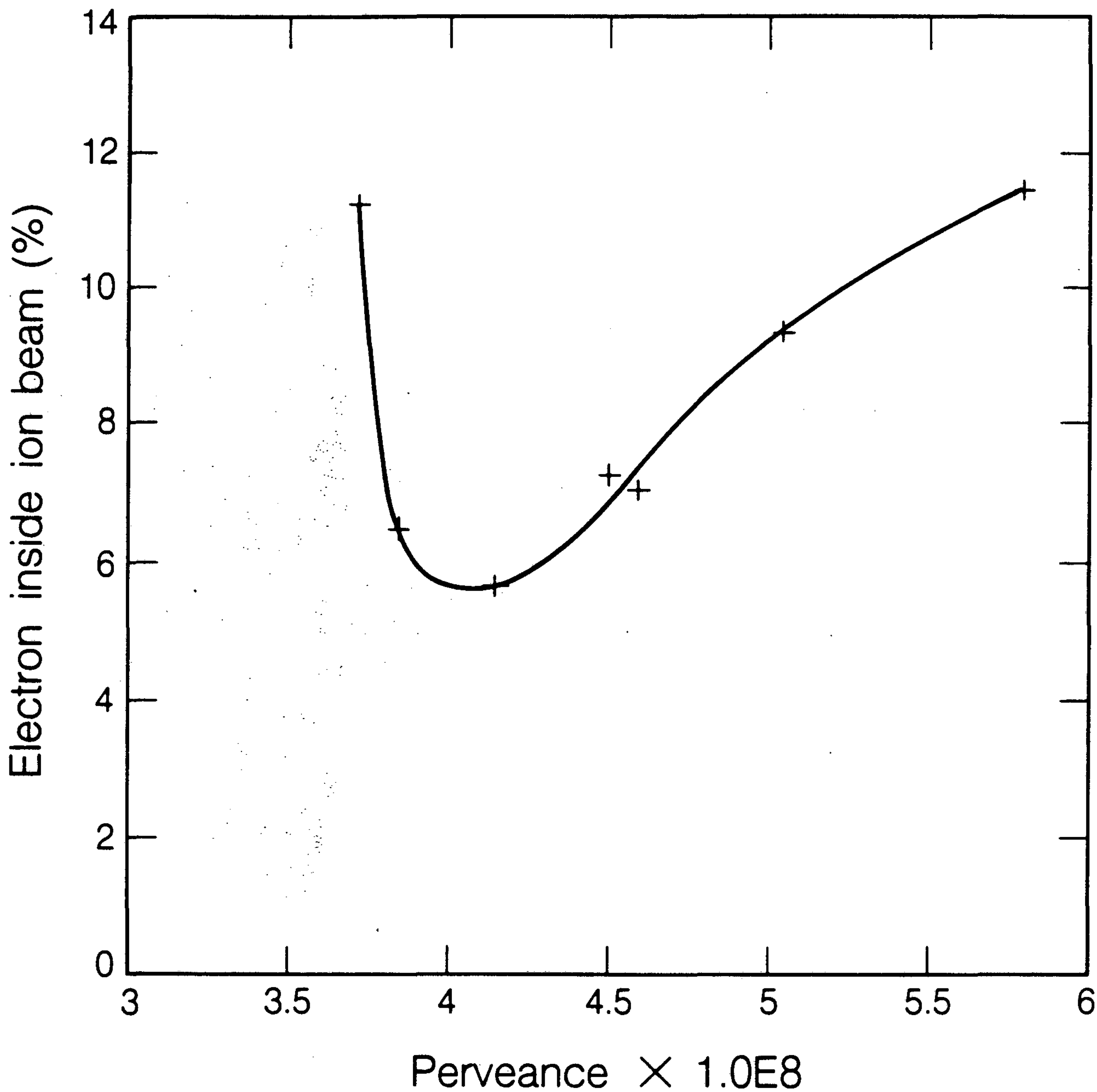

XBL 859-3813

Fig. 15

LAWRENCE BERKELEY LABORATORY
TECHNICAL INFORMATION DEPARTMENT
UNIVERSITY OF CALIFORNIA
BERKELEY, CALIFORNIA 94720